

MUTUAL SHADOWING AND DIRECTIONAL REFLECTANCE OF A ROUGH SURFACE: A GEOMETRIC-OPTICAL MODEL

Xiaowen Li, Alan H. Strahler
Center for Remote Sensing, Boston University

ABSTRACT

It has been shown that mutual shadowing, which induces a spatial correlation between illumination and viewing directions, plays an important role in modeling the BRDF of a rough surface consisting of large primary grains such as forest tree crowns [1]. This paper describes a Monte Carlo simulation of these mutual shadowing effects. Some new results of these simulations and the corresponding modeling efforts are also presented. For example, simulation results show that our simple assumption that all illumination shadows will preferentially occupy the lower surface of crowns is not realistic enough and may cause a considerable discrepancy between modeled results and simulation. Therefore, we have modified our model accordingly. This was accomplished by making the probability that a point on the surface of the crown is illuminated to be a function of height from the base of the crown, while still accounting for the fact that at the hotspot the probability that all illuminated points are viewed is one. With this change, modeled results show better agreement with the simulations. Forest BRDFs and BRFs as inferred or observed from real data often show a sharp rise at the edge of the "bowl," especially at large zenith angles opposite to the sun position. Modeled results do not always match this behavior. For example, our modeled BRDFs for dense stands remain high and flat at high view zenith angles because once a certain view zenith is reached, only sunlit crown is visible. Since the proportions don't change with further increase of zenith angle, the BRDF remains constant. The remedy for this is the introduction of a specular lobe in the reflectance function for a sunlit crown.

INTRODUCTION

The spatial correlation of mutual shading effects in viewing and illumination directions plays an important role in the bowl-shape of the observed BRDF of discrete element canopies [1]. In our model, mutual shadowing effect of primary grains is described first for two extreme cases: 1) all grains are centered at the same height ("Uniform Case"); and 2) they are randomly distributed over such a large range of heights ("Random Case") that any surface element may get shaded independently in illumination and view directions. A structural parameter β is used to describe situations between these two extremes. Two quantities were found important for describing the mutual shadowing effect in the Uniform Case (UC): $P_i M_i$ and $P_v M_v$, where M_v is defined as the mutual shadowing proportion of grain surface in the view direction; P_v is defined as the probability of this this proportion facing illumination. P_i and M_i are defined in the same way with two direction interchanged. In addition, P_o is defined as the proportion which is mutually shaded in both directions.

In order to further validate our model and better understand the mechanism, we have done more Monte Carlo simulations for different canopy structures and illumination conditions. From the simulation results so far, we can conclude that:

1. For UC on PP (Principal Plane), it is quite accurate to model $P_o = P_i M_i$ at $\theta_v > \theta_i$; and $P_o = P_v M_v$ at $\theta_v < \theta_i$, until the large zenith in the forward direction is reached where $P_v M_v > P_i M_i$ again. This suggests that we can directly model $P_v M_v$ and $P_i M_i$, rather than model all M_i , M_v , P_i , P_v , hence some difficulties we had before can be avoided.
2. The M_i boundary defined in our model should be "fuzzier".
3. For UC on places off-PP, a cosine function of azimuth can fit A_c (proportion of both illuminated and viewed surface) better than linear function previously used in our model.
4. The "Random Case" (RC) hardly exists for spheroid shaped primary grains, because the top layer plays more significant role in determining the bowl-shape. A wide range of realistic structures can be approximated as UC with good accuracy. A "probability weighted overlap area" is used to derive a new index β which is mathematically more robust than the one we used before.
5. Simulations show that for a given (large) coverage, the variance of $A_c(\phi)$ for a given viewing zenith angle may be a good indicator of the height variation of crown centers, as well as crown size. The larger viewing zenith angle, the better this indicator will be, since the less common parts of crowns can be viewed at all azimuth. A possible advantage of this approach may be its relative independence to background variation.

Our work presented here is a further step in pursuing geometric-optical modeling of BRDF over a vegetation canopy consisting of crowns [1]. Since we treat crowns as opaque primary grains and such grains are allowed to overlap freely, our model can be used to calculate the BRDF of any rough surface which can be modeled with similar free overlapping opaque primary grains. A possible advantage of our model is that the spatial correlation of the surface of such primary grains is taken into account. In other geometric-optical models of rough surface, such as the Beckman-Spizzichino model or the Torrance-Sparrow model (cited in [2]), where the surface is described as independent small facets, and the mutual shadowing is only described by a density distribution or normal-vector distribution along height, the spatial correlation among these facets are ignored.

ALGORITHM

Our Monte Carlo simulation program first generates 3-D random locations of the centers of spheroids according to the given parameters: mean crown radius R , mean height h of crown centers, ratio b of vertical axis over horizontal axis of the spheroid, and the distribution range of crown center in height. We assume it is uniformly distributed from h_1 to h_2 . We keep the ratios R/h and b constant for all crowns, thus the higher a crown center is, the larger the crown. Then, the program performs a linear transform in the vertical direction so that all the spheroids will look like spheres, the given zenith is also transformed to θ' at the same time. This is only for the convenience of calculation, as we explained in [1]. Later works are all done in this transformed 3-D space.

Then the program calculates and stores the area, location, and orientation of flat surface elements conforming to the surfaces of each spheroid using a given step size in a spheroid coordinate system originating at the center of the crown. This accomplished, the program calculates the surface normal of each element, and if the dot-product $\langle s, i \rangle$ of its normal and illumination direction is negative, the element is classified as an element "facing away from the sun." Otherwise, the program calculates whether it is in the illumination shadow of any other crown. This is achieved by first calculating whether a surface element is inside (intersected by) other crowns, and if not, a ray-tracing algorithm is used to see whether it is obstructed by other crowns along the given direction (in this case, the illumination direction). Then the whole crown surface is classified into four categories: facing away, free of mutual shading, intersected, and mutual shaded.

Border effects are handled by projecting the shadows of the far edge to the near edge. This is equivalent to repeating the crown center distribution pattern in all neighbouring pixels in our program.

Keeping the classification of all surface elements of this crown recorded, the above procedure is repeated for a given viewing direction. Each surface element is again classified into four viewing categories, resulting in 16 combined categories. The total surface area, as projected to viewing direction, is accumulated for each category.

Finally, the above procedure is repeated for every crown, and we get the total areas of all 16 categories of crown surface in the pixel at a given illumination and viewing direction. The program then prints out the total crown surface area, as projected to the sensor, and the proportion of area in each category in this total.

In order to better understand cases other than PP and principal cone as in [1], the program has been changed to give the simulation results along an arbitrary azimuth, changing viewing zenith from $90^\circ - \Delta\theta_v$ to nadir, at step $\Delta\theta_v$. For the case of 30 crowns in a pixel, a Sparc station needs about an hour to get the result for a given azimuth at $\Delta\theta_v = 2^\circ$ and crown surface splitting to 90×90 elements. When the number of crowns is 120, the algorithm will take about 8 hours on a Sparc workstation for a given viewing azimuth. In order to do more simulations, we have further rewritten the program into C++, so that the simulation can be run on a supercomputer Connection Machine (CM) which has 64k parallel processors. By simply spreading the surface elements of a crown into parallel processors, the computing time is reduced from 8 hours on a Sparc to a few minutes on CM.

Thus far, several different parameter sets have been used for simulations. Time and space prevent us from presenting all the results here. We will give only one example for each of our conclusions listed previously.

The "default" parameter set is the same one used in [1]. That is, a density of 30 crowns of 3-m radius per 900 m² area, a crown shape ratio $b/R = 1.5$, $b/h = 0.18$, and a constant canopy height $h = 25$ m. Vertical coverage for this example is $1 - e^{-\lambda\pi R^2} = 0.61$. The illumination zenith angle is taken as $\theta_i = 30^\circ$.

Figure 1 shows $P_v M_v$, $P_i M_i$ and P_o varying with zenith on PP. We can find that modeling $P_o = P_i M_i$ at two ends and $P_o = P_v M_v$ in middle on PP curve is quite accurate, so we almost can't find the third curve.

Hence we may think $P_v M_v + P_i M_i - P_o$ is the curve on the top. Though the $P_v M_v + P_i M_i - P_o$ calculated from model in [1] catches the basic pattern of this top curve, the agreement needs to be improved. By analysis of simulation results, we can easily identify the disagreement as being that our assumption for the "M_i boundary" is too strict, and real boundary is much fuzzier.

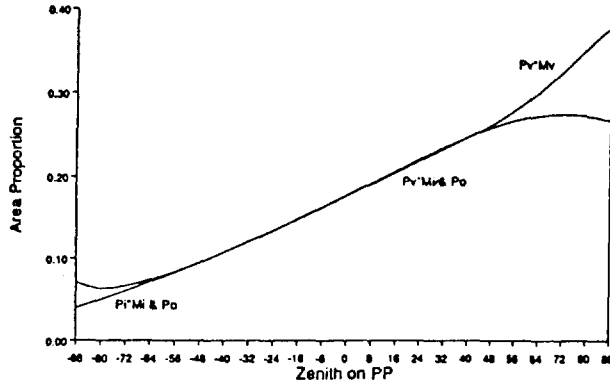


Fig. 2 shows $A_c(\phi)$ can be better fitted by a cosine function rather than a linear.

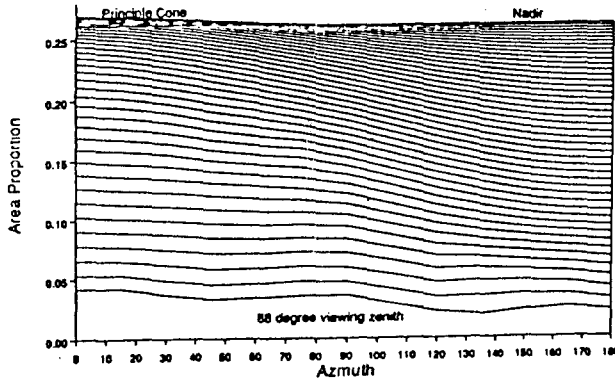
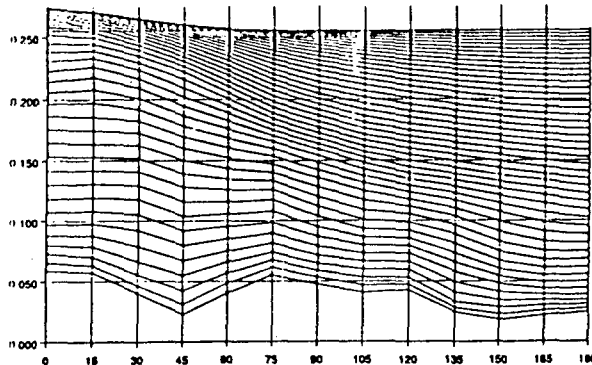


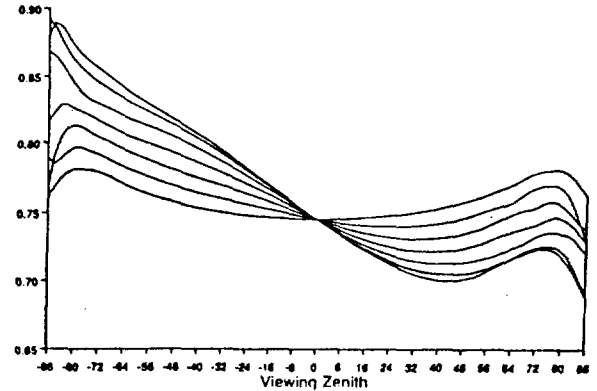
Fig. 3 shows $A_c(\phi)$ when the height distribution range is $25m \pm 20\%$. In comparison with Fig. 2, note that the bowl shape decreases with height variation (e.g. the curve for $\theta_v = 88^\circ$). It is clear that at the small zenith, more crowns contribute to $A_c(\phi)$ then the curves are more regular, while at larger zenith, only few top layer crowns will contribute then greater randomness.



These simulations confirm the difficulty in clearly defining a top layer independent to illumination and viewing geometry when the crown centers are randomly distributed in height. On the other hand, this may also offer us a new approach to reveal the 3-D structure of forest. Of course it will be very difficult: the greatest correlation between the height variation and variance of $A_c(\phi)$ occurs at large zenith, where SNR is the lowest.

In many natural forests, there may be physically clear-defined layers. Such case can be handled relatively easily by G-O model, by recursively treating the BRDF of lower layer as background of upper layer. Simulations also suggest that the definition of the top layer has to consider both coverage and variation in height. The higher the coverage, the thicker of crowns can be treated as a single layer. The lower the coverage, the thinner the top layer will be.

In order to evaluate possible specular reflectance components, we further modified the simulation program so that the norm of each surface element of A_c can be in some way recorded. At present, we weight each surface element by the cosine of the angle between the norm of surface element and the ideal norm direction which may yield specular reflectance, and accumulate all such elements, calling the ratio of the weighted sum over A_c the "specular index", (Fig. 4). This may not be the best way to evaluate the specular effect, but before we have more knowledge about such components of real crown, such an index may still give us a hint. Simulation results shows that it may explain why at large zenith angles the bowl edge rises much higher than a lambertian reflectance of crown surface could, especially at the azimuth opposite to the sun.



MODELING A_c

As revealed by the Monte Carlo simulation, even in UC, the illumination shadows do not all fall below M_i boundary. This makes accurate modeling more difficult. Modeled mutual shadowing is systematically less than that simulated in a wide, important range, which is basically governed by $M_i P_i$ in UC.

In order to improve the accuracy, we need to make the M_i boundary fuzzy. In [1], M_i indicates the mean probability of the hemisphere facing the sun to be mutually shaded by other crowns. A strict M_i boundary means that all points under the M_i boundary have a probability equal to one to get mutual shadowing, while all points above the boundary have a probability of zero. In order to model a fuzzy boundary, we need to consider the probability of a point on the illuminated hemisphere more realistically. We have obtained the probability that a point z on the illuminated half of spheroidal surface in UC will be free from mutual shadowing:

$$p_z = e^{-\lambda \Gamma_z}, \quad (1)$$

where Γ_z is the shaded area on a horizontal plane passing z , cast by the part of spheroid above the point; λ is the counts density of spheroids. Knowing p_z , we can obtain:

$$P_i M_i = 1 - \int p_z \frac{\langle s, v \rangle ds}{(0.5(1 + \langle i, v \rangle))}, \quad (2)$$

where ds is spheroidal surface element facing both illumination and viewing direction v ; s is the surface normal of ds .

The numerical integration according to the above formulas agrees with the simulation results fairly well, see Fig. 5. This better agreement proves that the strict M_i boundary is the major limitation of the formulas used in [1]:

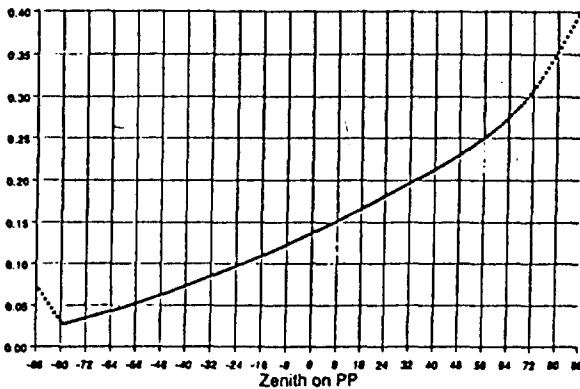
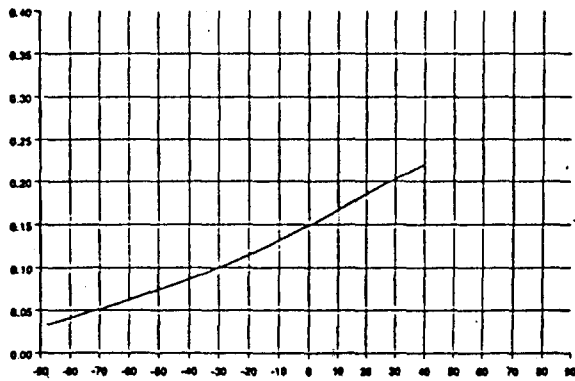
$$P_i M_i = (1 - \cos(\theta_{M_i} - (\theta'_i - \theta'_v \cos \phi))) / 2; \quad (3)$$

$$P_v M_v = M_v - (1 - \cos(\theta'_v \cos\phi - \theta'_i)) / 2, \quad (4)$$

where θ_{M_i} is an angle indicating the size of a strict M_i slice. However, since eqs. (3) and (4) have already caught the basic characters of the simulation, and numerical integration is not as easy and understandable as simple approximation, we prefer to use (3) and (4) as basic frame of our modeling. The basic idea is to define a fuzzy factor to extend the M_i boundary, such an extension should reflect some basic characters of simulations and eqs. (1), (2), which suggests the weaker the mutual shadowing, the fuzzier the M_i boundary, and vice versa. Secondly, such an approximation should guarantee the right result at the hotspot. The following simple modification is finally adopted after the comparison of a few possible choices:

$$P_i M_i = (1 - \cos(\theta_{M_i} (1 - (\theta'_i - \theta'_v \cos\phi) / \pi))) / 2. \quad (5)$$

This implies that the slice between M_i and viewing boundaries contains only θ_{M_i} / π of shadow, remaining shadow may be cast above M_i boundary. This formulation guarantees that 1) at the hotspot, $P_i M_i = M_i$; 2) the larger M_i , the less fuzzy the boundary would be; 3) πM_i goes to zero only when $\theta'_v - \theta'_i \cos\phi$ gets π . Using eqs (4) and (5), the result is shown in Fig. 6.



PRACTICAL HEIGHT DISTRIBUTION CASES

In [1], we have modeled realistic cases as linear combination of extremes UC and RC. The interpolation weight β used there is somewhat intuitive and arbitrary. Though it agrees with simulation results reasonably well so far, it depends on the height distribution range only, and has totally ignored the effect of coverage. This may cause some theoretic inconsistency or significant error in some special cases. Thus we need to get a more mathematically sound solution.

In order to achieve this, we first need to obtain a $\Gamma(h, z)$ similar to th Γ_v above but one which also includes the viewing shadow and overlap function at height z of a spheroid centered at height h . Since plane z is allowed to intersect the spheroid, the expression will be very tedious.

Fortunately, as we have observed from the simulation results, P_o is very close to $M_v P_v$ from hotspot to nadir and very close to $P_i M_i$ outward from hotspot. This implies that we can determine $\Gamma(h, z)$ by θ'_i only from hotspot to nadir; by θ'_v only outward from hotspot. On the other half on the PP opposite to sun, the overlap area of $\Gamma(h, z)$ will be a circle.

With this approximation, similarly to eq. (1) and (4) in [1] we can obtain a shadow function $\Gamma(h, z) = \Gamma_i(h, z) + \Gamma_v(h, z) - O(h, z)$.

Given the height distribution of centers, the variation of average overlap function $O(z)$ at z may be conceptually important for us to better understand the difference between UC and practical cases. In the UC, at near the tops of crowns:

$$\Gamma_i(h, z) = \Gamma_v(h, z) = O(h, z),$$

the situation is just like it always is at hotspot, where the same equality holds. When z gets lower, $O(h, z)$ in $\Gamma(h, z)$ will get smaller. However the probability of a crown surface being illuminated also gets smaller and hence this smaller $O(h, z)$ will play less significant role in the BRDF. Thus the bowl-shape can be understood in the same way as the hotspot when only tops of crowns which satisfy $\Gamma_i = \Gamma_v = O$ dominate. By the same token, we may introduce the "Probability Weighted Overlap Function" at nadir viewing for describing practical cases. We define:

$$\beta = \frac{\int_{h_1}^{h_2} O(h) e^{-\lambda(h) \Gamma_i(h)} d\lambda(h)}{O(0,0) \int_{h_1}^{h_2} e^{-\lambda(h) \Gamma_i(h)} d\lambda(h)}, \quad (6)$$

where $\Gamma_i(h)$ is defined similarly as $O(h)$, i.e. the average shadowing areas at level h , of all the crowns which may cast shadows on that level, $\lambda(h)$ is the accumulation distribution of crown counts. If we further assume $d\lambda(h)/dh$ is constant within range h_1 to h_2 and zero outside, we may use a simple approximation: $O(h) = O(0,0) e^{-(h-h_1)D}$, where the correlation depth of a single crown at nadir viewing is: $D = R \cos(\theta_i/2)$. Then eq.(6) can be analytically solved:

$$\beta = \frac{\lambda \Gamma_i}{\lambda \Gamma_i + (h_2 - h_1) D} \frac{1 - e^{-\lambda \Gamma_i - (h_2 - h_1) D}}{1 - e^{-\lambda \Gamma_i}}. \quad (7)$$

This equation is simple but it reasonably reflects almost all factors which determine the canopy structure and illumination geometry, though the values derived from it are not significantly different from those from [1] for all our simulations and for seven forest sites where our BRDF model validation is in process.

Reference

- [1] X. Li and A. H. Strahler, Geometric-Optical Bidirectional Reflectance Modeling of the Discrete-Crown Vegetation Canopy: Effect of Crown Shape and Mutual Shadowing, IEEE Trans. on GARS, 1992, in press.
- [2] S. K. Nayar, et. al., Surface Reflection: Physical and Geometrical Perspectives, IEEE Trans. on Pattern Analysis and Machine Intelligence, Vol. 13, No.7, p611-634, July 1991.

ACKNOWLEDGEMENTS

This research was supported in part by NASA grant NAGW-2082 and NASA contract NAS5-30917, as well as National Natural Science Foundation grant 4880050.